Understanding hammerscale: the use of high-speed film and electron microscopy

David Dungworth and Roger Wilkes

ABSTRACT: Hammerscale is the product of high-temperature oxidation of iron alloys and it is particularly associated with the forging of iron. Due to its magnetic properties hammerscale is easily recovered from archaeological contexts. While most hammerscale consists of flakes of iron oxide, a small proportion consists of spheres. This paper presents the results of the microscopic examination and chemical analysis of both flake and spheroidal hammerscale from archaeological contexts as well as material recovered during experimental forging and welding. In addition, the experimental fire-welding of iron has been recorded using high-speed digital video. This demonstrates that spheroidal hammerscale is produced during forge welding. The chemical analysis of the experimental hammerscale shows that it is formed from oxidized iron with a small but significant contribution from the non-metallic inclusions in the metal.

Introduction

Hammerscale is a shiny, black, magnetic waste product which forms during the hot working of iron and its alloys. It is usually encountered as small plates, sheets or flakes several millimetres across and less than a millimetre thick (Fig 1). Archaeological samples of hammerscale usually contain a small proportion of spheroidal material (Fig 2). It has been suggested that these spheroids can be produced by several different iron-working processes including bloomery iron smelting, primary consolidation of bloomery iron, and fire-welding of iron. This paper presents the results of the examination and analysis of archaeological specimens of flake and spheroidal hammerscale. In addition we have carried out forging and welding experiments and reproduced both types of hammerscale.

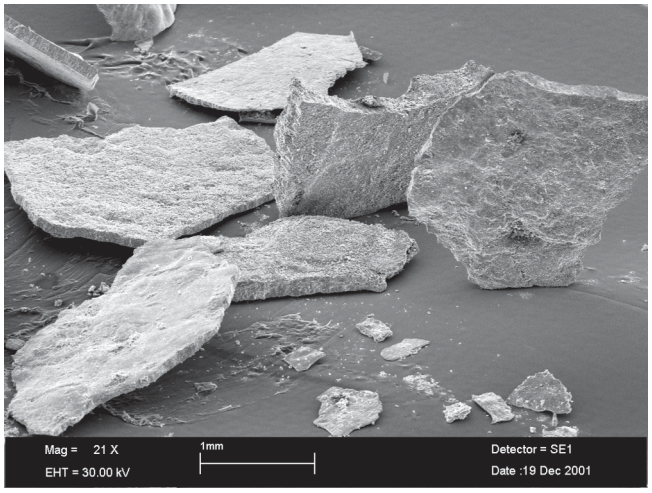

Figure 1: Secondary electron image of flake hammerscale from Mont Beuvray, France.

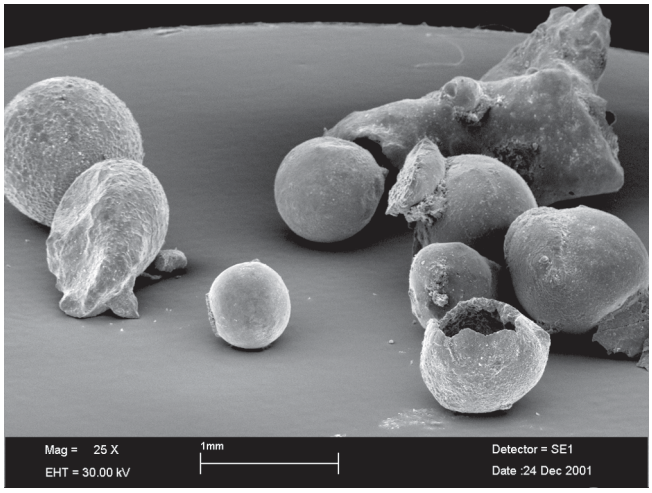

Figure 2: Secondary electron image of spheroidal hammerscale from Mont Beuvray, France.

Previous studies of hammerscale

Early 20th-century archaeological excavations of blacksmiths' workshops (*eg* Forster and Knowles 1910; 1913) often refer to the presence of smithing hearths, as well as scrap metal and part-made objects. Less frequently, these early reports describe the occupation horizon within these workshops as black. While with hindsight we can suggest that these layers were probably rich in hammerscale, the modes of excavation and recording then used did not allow its recognition.

The earliest explicit recognition of hammerscale in archaeological literature in England comes from the report of an excavation of the Roman fort of Benwell on Hadrian's Wall (Simpson and Richmond 1941). The excavators were intrigued by the presence of a black layer and sent samples of this to Smythe who carried out chemical analysis that showed,

> 'In the main, the material is the magnetic oxide of iron, Fe_3O_4, containing ferrous oxide in considerable amount and some metallic iron. There can be no doubt that it is a mill-scale or smithy scale, and that the deposit is derived from the sweepings of a black smiths shop' (Smythe in Simpson and Richmond 1941, 41).

The excavation of a Roman iron-smelting site at Ashwicken, Norfolk (Tylecote and Owles 1960) revealed large deposits of hammerscale. The examination of a cross-section through a sample of hammerscale showed that it 'contained 85.8 per cent of magnetite, the remainder being cementing films of fayalite' (*ibid*, 149, fig 9). Tylecote (1962, 254) described hammerscale as forming during the heating and forging of iron and suggests that several different oxides of iron may be formed, including ferrous iron oxide (FeO), magnetite (Fe_3O_4) and ferric oxide (Fe_2O_3). He also proposed that most of the silica in the cementing films derived from the slag inclusions in the iron and possibly from the use of sand as a flux (*ibid*, 255).

McDonnell (1984) identified two types of hammerscale on the basis of their shapes: flakes and hollow spheroids. He observed that flakes of hammerscale were much more abundant than spheroids. Cross-sections of both types of hammerscale were examined with a scanning electron microscope and the chemical compositions determined using an energy dispersive X–ray spectrometer. He concluded that both types had similar microstructures but that the spheroids, which were often hollow, contained more phosphorus. Subsequently he suggested that the spheroids were produced during the fire-welding of iron and that a sand flux was important in their formation (McDonnell 1986). He proposed that the oxidized surface of the iron and the sand flux would react together. When two pieces of metal were welded together, the heat and the pressure combined to extrude this slag which would then be 'cooled in flight' (*ibid*, 146).

Allen (1986) described in detail the morphology of hammerscale and related debris recovered from an eroding section on the edge of the river Severn. The material probably derived from a Roman-period workshop where blooms were consolidated into bars. Allen identified twelve different types of hammerscale on the basis of their size and shape but it is clear that flakes were the most common type and the others made up a very small proportion of the assemblage.

Unglik (1991) examined a large quantity of hammerscale from an early 19th-century blacksmithy in Canada. This assemblage included both flakes and spheroids: the former averaged 0.3mm in thickness while the latter averaged 2mm in diameter, with 66% of them being hollow. Samples of each were mounted in cross-section for an examination of their microstructures. Both types of hammerscale were found to be composed of magnetite and wüstite crystals, with a fayalite bonding. Unglik found that some of the spheroids had highly dendritic iron oxide (implying a rapid cooling rate) while the flakes often had a 'featureless oxide scale structure' (1991, 96).

Sim (1998) examined Roman hammerscale from Silchester and produced hammerscale during the experimental replication of many iron smithing activities. The experiments demonstrated that most hammerscale consists of flakes and that these were deposited close to the anvil. The examination of the experimentally produced hammerscale showed that small quantities of spheroidal hammerscale were produced during welding. Limited chemical analyses were undertaken which revealed that all samples were rich in iron oxide and silica but that the iron oxide to silica ratio varied depending on the metal being worked. Well-refined billets gave hammerscale with a high iron oxide content while less well-refined iron gave hammerscale richer in silica.

Hammerscale is now routinely recovered from archaeological soil samples (Bayley *et al* 2001). Flake hammerscale is the most abundant form and there is no doubt that it forms due to the partial oxidation of the surface of iron as it is heated in a hearth prior to

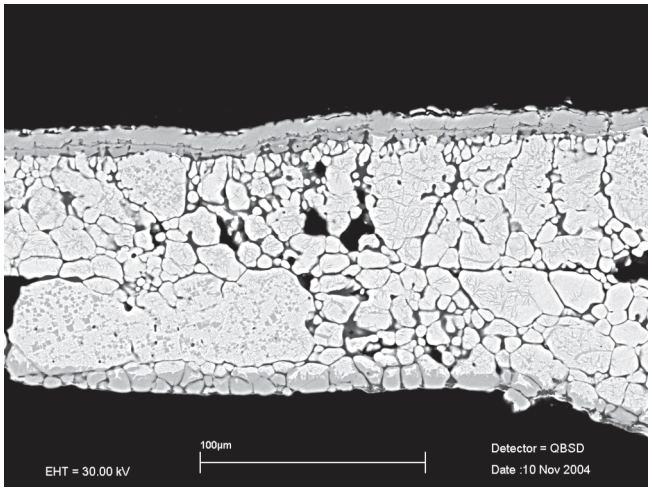

Figure 3: Backscattered electron image of a cross-section through sample A2 (flake hammerscale from Mont Beuvray) showing the dominance of iron oxide (white) with some fayalite or glassy material (mid grey) along grain boundaries.

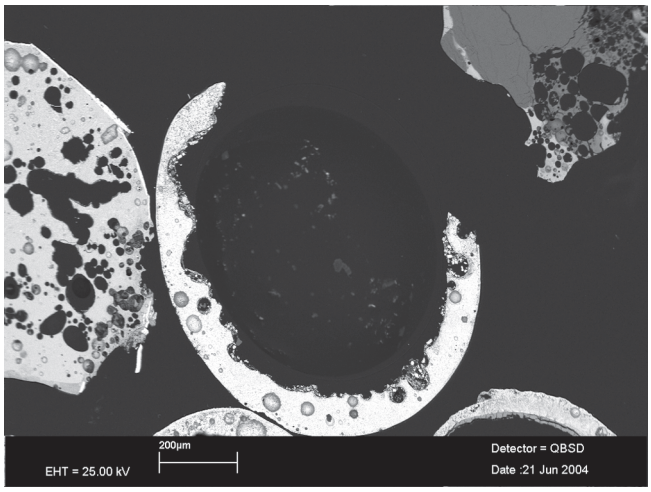

Figure 4: Backscattered electron image of a cross-section through sample A8 (spheroidal hammerscale from Mont Beuvray).

smithing. When the hot iron is struck with a hammer, the relatively soft iron plastically deforms while the brittle scale on the surface flakes off and is deposited around the anvil. Spheroidal hammerscale has been recognized from archaeological contexts for several decades but its origins are less well understood. It is widely accepted that spheroids, which are often hollow, were molten and have cooled rapidly. The most popular hypothesis for its formation is fire-welding. It is assumed that the combination of temperature and pressure is enough to first melt the two layers of scale present in a weld, and then eject the oxides as a liquid which forms spheroids as it travels through the air.

Examination of archaeological samples

Twenty samples of hammerscale were obtained from two archaeological sites, Mont Beuvray and Hythe Hill. Mont Beuvray, France (ancient *Bibracte*) is a late Iron Age (1st century BC) *oppidum* in central France (Guichard *et al* 2003). The excavation of a blacksmith's workshop (CP11bis) within the *oppidum* was accompanied by the collection of hundreds of soil samples taken on a grid following the methodology described by Mills and McDonnell (1992). The excavation of a late medieval (15th- or 16th-century) smithy at 79 Hythe Hill, Colchester (Brooks 2000) recovered substantial quantities of smithing pan, consisting of a floor deposit of hammerscale cemented together. Five samples of flake and spheroid hammerscale were selected from each site. The samples were mounted in epoxy resin and polished to expose a cross-section. The samples were examined using a scanning electron microscope (SEM) and the chemical composition determined using an attached energy dispersive X-ray spectrometer (EDS). All elements detected were calculated stoichiometrically as oxides; iron was calculated as Fe_3O_4 in all cases and, while it is likely that the valence state of iron varies through the samples, this will have a limited impact on the quantitative results presented here. Three to six areas of each samples were analysed (the number of areas depending on the heterogeneity of the sample), each result was normalized to 100wt% and then averaged.

Flake hammerscale

The samples of flake hammerscale from both sites are composed almost entirely of large, euhedral grains of iron oxide, with a very small amount of fayalite and/or glass along the iron oxide grain boundaries (Fig 3). In most cases the iron oxide grains are probably magnetite but the back-scattered SEM images show occasional differences in brightness which probably reflect the fact that some of the iron oxide is present as wüstite and/or haematite. The arrangement of the iron oxide grains in the flake hammerscale often shows a series of layers. Calculated as magnetite, the iron oxide content of these samples always exceeds 92wt%; the balance is mostly silica and alumina (Table 1).

Spheroidal hammerscale

All of the samples of spheroidal hammerscale displayed some porosity and many were completely hollow (Fig 4). The samples have a microstructure consisting of fine dendrites of iron oxide in a matrix of fayalite and/or glass (Fig 5). The proportion of fayalite and/or glass in the spheroids is higher than that seen in the flakes and these samples generally have lower concentrations of iron oxide compared with the flake hammerscale (Table 2).

Table 1: Average composition of flake hammerscale samples from archaeological contexts (A1–5 = Mont Beuvray, A11–15 = Hythe Hill).

	Na_2O	MgO	Al_2O_3	SiO_2	P_2O_5	SO_3	K_2O	CaO	TiO_2	MnO	Fe_3O_4
A1	<0.1	<0.1	0.7	0.7	<0.1	<0.1	0.1	<0.1	<0.1	<0.1	98.5
A2	<0.1	<0.1	2.2	4.6	<0.1	<0.1	0.3	<0.1	<0.1	<0.1	93.0
A3	<0.1	0.3	2.5	3.5	0.5	<0.1	0.2	0.6	0.1	<0.1	92.2
A4	<0.1	<0.1	0.2	0.2	0.1	<0.1	<0.1	0.1	<0.1	<0.1	99.2
A5	<0.1	<0.1	1.2	2.5	0.3	<0.1	0.2	0.4	<0.1	<0.1	95.5
A11	<0.1	<0.1	0.5	2.5	0.3	<0.1	<0.1	0.2	<0.1	<0.1	96.4
A12	<0.1	<0.1	0.2	0.2	<0.1	<0.1	<0.1	0.2	<0.1	<0.1	99.4
A13	<0.1	0.1	1.0	2.8	0.1	<0.1	0.1	0.4	<0.1	<0.1	95.4
A14	0.3	<0.1	0.4	1.1	0.9	<0.1	0.1	0.7	<0.1	<0.1	96.4
A15	<0.1	<0.1	0.4	0.5	<0.1	<0.1	<0.1	0.1	<0.1	<0.1	98.9

Table 2: Average composition of spheroidal hammerscale samples (A6–10 = Mont Beuvray, A16–20 = Hythe Hill).

	Na_2O	MgO	Al_2O_3	SiO_2	P_2O_5	SO_3	K_2O	CaO	TiO_2	MnO	Fe_3O_4
A6	<0.1	<0.1	2.0	6.4	0.2	<0.1	0.2	0.1	<0.1	<0.1	91.1
A7	<0.1	<0.1	2.9	7.4	0.4	<0.1	0.3	0.1	<0.1	<0.1	88.9
A8	<0.1	<0.1	2.7	7.4	0.4	<0.1	0.2	0.2	<0.1	<0.1	89.1
A9	<0.1	<0.1	5.7	13.8	0.3	<0.1	1.1	0.9	<0.1	0.1	77.9
A10	<0.1	<0.1	2.3	6.4	0.1	<0.1	0.3	<0.1	<0.1	0.5	90.4
A16	<0.1	<0.1	0.6	3.5	0.4	<0.1	0.1	0.5	<0.1	<0.1	94.9
A17	0.7	0.6	5.7	16.8	0.4	<0.1	1.4	0.8	<0.1	<0.1	73.6
A18	0.4	0.2	6.1	19.3	0.4	<0.1	1.9	0.9	0.1	<0.1	70.6
A19	<0.1	<0.1	0.8	3.7	0.3	<0.1	0.2	0.2	<0.1	<0.1	94.8
A20	<0.1	0.3	3.4	18.4	0.4	<0.1	0.9	1.5	0.2	<0.1	75.0

Discussion of archaeological hammerscale

The examination of archaeological hammerscale samples shows that flake hammerscale consists almost entirely of euhedral grains of iron oxide with a small amount of fayalite or glassy material along grain boundaries. This microstructure is compatible with a model in which the iron oxides grow on the surface of the iron, both being solid. The spheroidal hammerscale is often hollow and consists of fine iron oxide dendrites in a fayalite or glassy matrix. This microstructure is compatible with a model of formation in which the spheroids start as a liquid and solidify during flight. There are no significant differences in the microstructures or chemical compositions of the two types of hammerscale when comparing between the two sites.

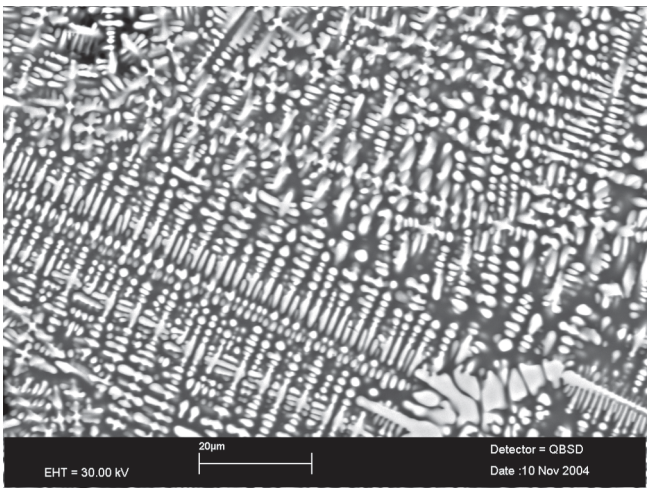

Figure 5: Backscattered electron image of a cross-section through sample A9 (spheroidal hammerscale from Mont Beuvray) showing dendrites of iron oxide (white) in a fayalite or glassy matrix (mid grey).

The compositions of the archaeological samples of hammerscale show correlations between most oxides (*eg* Figs 6 and 7). These correlations provide information about the role of other materials in the formation of hammerscale. Clearly the most important input is from the metallic iron, but slag inclusions in the metal, silica from any sand flux used, ash from the fuel used (assumed to be charcoal), and clay from the hearth lining may also contribute. Tables 1 and 2 show that a range of oxides are present in hammerscale and it is most unlikely that it is simply the product of oxidized iron and silica sand flux. It is possible that a complex mixture of oxidized iron, silica sand, fuel ash, and clay lining could produce chemical compositions similar to those seen in the

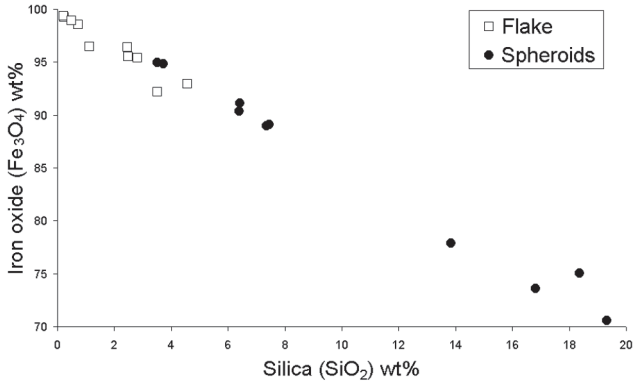

Figure 6: Silica v. iron oxide for archaeological hammerscale.

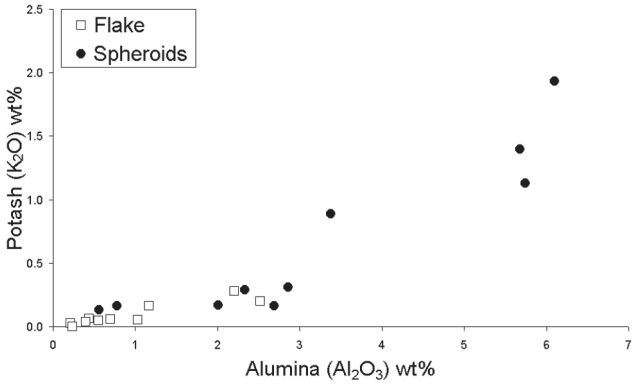

Figure 7: Alumina v. potash for archaeological hammerscale.

archaeological samples, which differ from those of the experimentally-produced hammerscale.

Replication experiments

A series of experiments was carried out to examine the types of hammerscale produced during forging and welding. The main aim was to provide unequivocal evidence that spheroidal hammerscale is produced during fire-welding. The experiments were undertaken using modern mild steel and a bar of 19th- or early 20th-century wrought iron produced by puddling. The wrought iron bar was retained to determine the sorts of non-metallic inclusions present; unfortunately a sample of the steel bar was not retained. The forging and welding were carried out in the teaching workshops of West Dean College, Chichester, under the supervision of a professional smith (Andrew Breese). The floor around the hearth and anvil (to a distance of 5m) was thoroughly cleaned before work started (although hindsight shows that cleaning was not complete). After each experiment the hammerscale was swept up and bagged (all material fell within 2m of the anvil). This material was subsequently sorted into flake, spheroidal and miscellaneous hammerscale (Table 3).

The blacksmith's hearth was of a modern type, constructed from sheet metal with a water-cooled cast iron tuyère (cf CSIRA 1952, 1–3, fig 2). The draught was provided by an electric blower and the fuel used was a metallurgical coke (samples of clinker were retained for analysis). One end of a bar of iron or steel (each 20mm square-sectioned bars) was forged down to a section approximately 10mm by 25mm and then bent

Table 3: Weights of hammerscale recovered from each experiment.

			Weight (g)			Percentage		
Experiment	Action	Metal	Flake	Spheroid	Miscell.	Flake	Spheroid	Miscell.
1	Forge	Iron	33.32	0.0006	0.95	97.2	0.002	2.8
2	Weld	Iron	2.36	0.21	1.84	53.5	4.8	41.7
3	Forge	Iron	15.29	0.74	0.52	92.4	4.5	3.1
4	Forge	Iron	5.27	0.05	0.05	98.1	0.9	0.9
5	Weld	Iron	3.28	0.19	0.98	73.7	4.3	22.0
6	Forge	Iron	38.34	0.73	3.68	89.7	1.7	8.6
7	Forge	Mild steel	3.21	0.05	0.09	95.8	1.5	2.7
8	Weld	Mild steel	5.61	0.22	0.04	95.6	3.7	0.7
9	Forge	Mild steel	3.36	0.10	0.15	93.1	2.8	4.2
10	Weld	Mild steel	5.04	0.17	0.33	91.0	3.1	6.0
11	Forge	Mild steel	3.93	0.11	0.44	87.7	2.5	9.8
12	Weld	Mild steel	2.25	0.28	0.37	77.6	9.7	12.8
13	Burn	Iron	0.00	1.93	0.00	0.0	100.0	0.0
14	Burn	Mild steel	0.00	1.11	0.00	0.0	100.0	0.0
15	Forge	Iron	4.54	0.15	0.58	86.1	2.8	11.0
16	Weld	Iron	1.87	0.41	0.27	73.3	16.1	10.6
Total			127.67	6.45	10.29	88.4	4.5	7.1

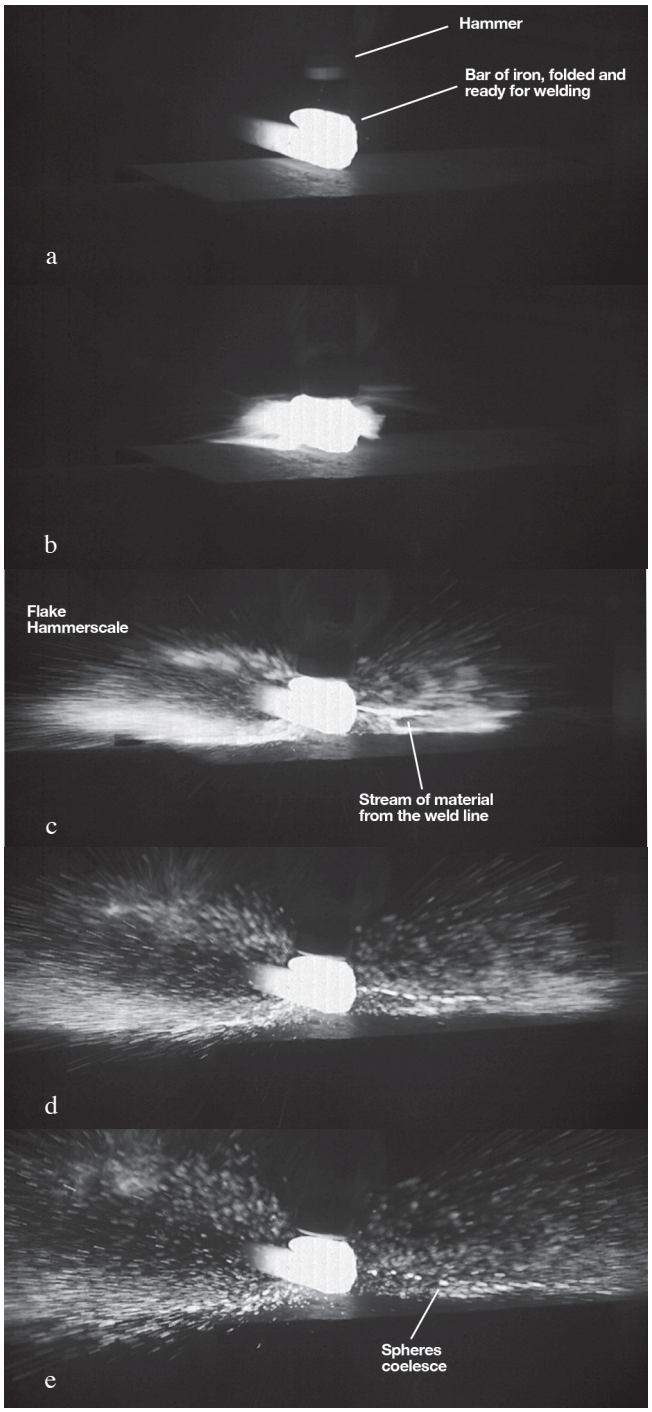

Figure 8: Five stills taken from the high-speed digital video of a weld (5/600ths of a second separate each image; a is the earliest). See text for discussion [see also back cover].

back on itself ready for welding. This required up to five separate periods of heating and forging. The welding was achieved by heating the prepared metal to a bright yellow heat and striking with a hammer (cf CSIRA 1952, 21). No fluxes were used during the forging or welding. The welded end of the bar was then forged down and bent back on itself in preparation for the next weld.

In total, 144.4g of hammerscale was recovered (Table 3); an unknown amount of hammerscale is likely to have been lost in the hearth during heating. With hindsight it is clear that it was not possible to keep the workshop floor completely clean and the method used to recover hammerscale (dust-pan and brush) was not ideal. The analysis of material collected after every stage of work indicates that a small proportion was contamination from earlier stages. Nevertheless, the weights of scale show that more spheroidal hammerscale was collected after each weld compared to the preceding forging stages. This is particularly apparent for the first forging and welding experiment which produced virtually no spheroids from the forging stage but 5% spheroids, 53% flake and 42% miscellaneous hammerscale from the succeeding welding stage. The examination of the three spheroids from stage 1 showed that two were contamination and one was a combustion sphere (see below).

A conventional digital video camera (25 frames per second) was used to record the action for the duration of all the experiments. In addition a high-speed digital camera (600 frames per second) was used to record several seconds of action for each welding experiment. A series of stills from this video are reproduced as Figures 8a–e (a copy of the video is available on YouTube: www.youtube.com/user/DDungworth). Figure 8c shows the weld 0.01 seconds after the moment of impact: most of the hammerscale is moving quickly away from the point of impact to produce a shower of sparks. In addition, a stream of bright material can be seen emerging from the weld line. The form of this material in this, and later frames, suggests that it is molten as it emerges from the weld line. In Figure 8d the stream of material starts to break up into smaller portions. This process is continued in Figure 8e where the material has coalesced into a series of spheroids.

The high-speed digital camera has successfully captured the formation of spheroidal hammerscale. This video confirms that spheroidal hammerscale is formed during welding. This process took less than 0.03 seconds and would not be observable without the aid of high-speed video.

In addition to forging and welding the wrought iron and mild steel, samples of both metal were deliberately over-heated until they began to burn. There was no control over the temperature of the burning; samples were simply heated until they began to resemble sparklers. The material which spontaneously fell off the metal, all of which was spheroidal, was collected in a container. These combustion spheroids are generally larger than the spheroidal material produced by fire-welding and subsequent examination (see below) showed this material

Table 4: Samples of hammerscale selected from the replication experiments for detailed analysis.

Samples	Experiment	Metal	Action	Type
E1–E6	1	Iron	Forge	Flake
E7–E9	1	Iron	Forge	Spheroid
E10–E15	1	Iron	Forge	Miscellaneous
E16–E21	2	Iron	Weld	Spheroid
E22–E24	2	Iron	Weld	Flake
E25	2	Iron	Weld	Miscellaneous
E26–E28	5	Iron	Weld	Miscellaneous
E29–E31	7	Steel	Forge	Spheroid
E32–E37	7	Steel	Forge	Flake
E38–E43	8	Steel	Weld	Flake
E44–E52	8	Steel	Weld	Spheroid
E53–E55	13	Iron	Burn	Spheroid
E56–E58	14	Steel	Burn	Spheroid

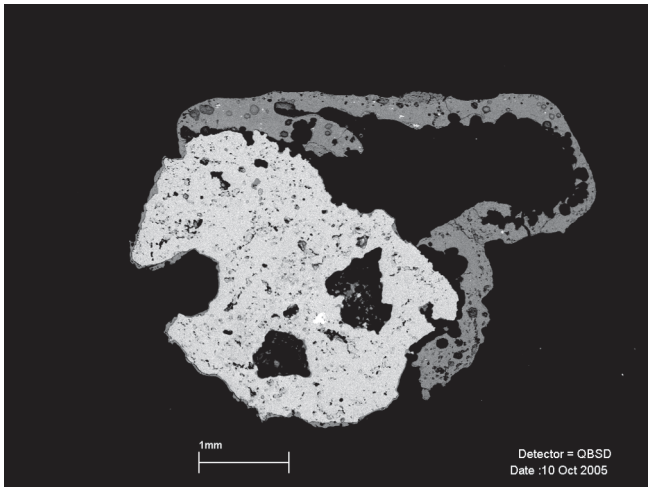

Figure 9: Backscattered electron image of a cross-section through sample E58 (spheroidal hammerscale produced by burning steel). Note the hollow shell is formed of iron oxide and iron silicate (mid grey) with a core of metallic iron (light grey).

has other distinctive features to. Given the problems with contamination among samples swept from the floor, the combustion spheroids provided the most secure samples and these are reported first.

Examination of experimental samples

A total of 58 samples of flake, spheroidal and miscellaneous hammerscale from forging, welding and burning of wrought iron and mild steel were selected for analysis (Table 4).

Combustion spheroids

Three spheroids were selected from the combustion both of mild steel and wrought iron (samples E53–E58). Their microstructure typically consisted of a small particle of porous but metallic iron 1–2mm across, surrounded by a film of oxidized material (Fig 9), quite distinct from those produced by welding. The metallic iron core was not observed in only one out of six cases, although this may simply reflect the problem of characterising a heterogeneous three-dimensional object using a single cross-section. Spheroids with a similar microstructure from earlier forging experiments (*ie* ones in which the metal was not deliberately burnt) are also interpreted as combustion spheres (*eg* E9, E30 and E31). The microstructure of the combustion spheroids resembles that observed by Starley for an example of Roman spheroidal hammerscale from Creeton Quarry (Starley 1997).

A striking aspect of the combustion spheres from the two metals is the fact that they have mutually exclusive chemical compositions (Table 5, the reported analyses are for the oxidized shell, not the metallic core). The wrought iron combustion spheroids contain significant concentrations of phosphorus and only low levels of manganese, but the reverse is true for the mild steel spheroids. As will be discussed in more detail below, the non-iron content of all types of hammerscale is heavily influenced by the non-metallic inclusions in the parent metal. In the case of the wrought iron these are rich in phosphorus while the inclusions in the mild steel are assumed to be rich in manganese.

Table 5: Averaage composition of the oxidized shell of the experimental spheroidal hammerscale samples produced by burning (combustion) of wrought iron (E53–55) and steel (E56–58).

	Na_2O	MgO	Al_2O_3	SiO_2	P_2O_5	SO_3	K_2O	CaO	TiO_2	MnO	Fe_3O_4
E53	0.4	0.2	2.6	12.4	1.3	2.6	0.1	0.3	0.2	0.2	79.8
E54	0.3	0.2	2.3	8.3	0.9	1.8	0.1	0.2	0.2	0.2	85.5
E55	0.5	0.2	2.5	8.2	0.9	1.8	0.1	0.2	0.1	0.2	85.2
E56	0.4	0.3	2.3	7.3	<0.1	2.2	0.1	0.3	0.1	1.8	85.2
E57	0.4	0.2	2.2	5.7	0.2	2.2	<0.1	0.3	0.1	3.7	84.9
E58	0.4	0.3	3.4	9.7	<0.1	2.1	<0.1	0.6	0.2	5.5	77.6

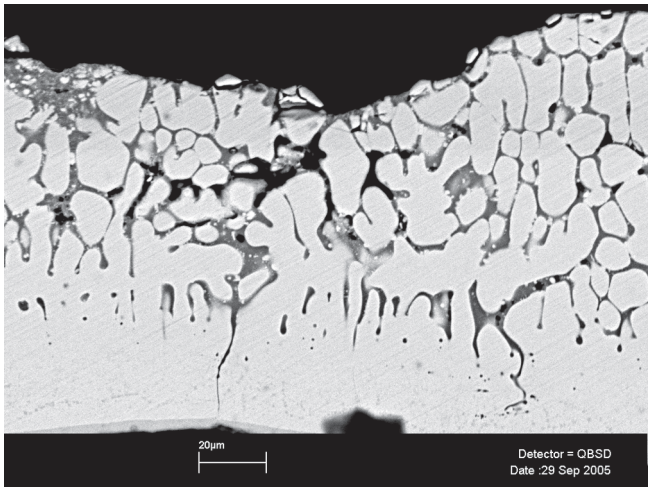

Figure 10: Backscattered electron image of a cross-section through sample E5 (flake hammerscale) from the forging of wrought iron.

Flake hammerscale

Twenty-one samples of flake hammerscale (E1–6, E22–24, E32–43) were selected from the forging and welding of both wrought iron and mild steel. They all displayed the same microstructure: relatively large grains of iron oxide (magnetite?) with small amounts of fayalite or glassy matrix along some grain boundaries (Fig 10). The iron oxide grains in many samples were arranged in layers which suggest that the flake hammerscale may have developed episodically. The microstructure of the flake hammerscale seems to be the same regardless of the material (mild steel or wrought iron) or the process (forging or welding). All of the wrought iron flake hammerscale samples contain appreciable amounts of phosphorus and negligible amounts of manganese while (with one exception) the reverse is true for the mild steel flake hammerscale (Table 6). This compositional difference is similar to that observed for the combustion spheroids. The one exception (E41) was collected after welding mild steel but it has a high phosphorus and low manganese content. We suggest this sample is contamination and that it would have been formed during an earlier experiment with wrought iron.

Spheroidal hammerscale

Twenty-one samples of spheroidal hammerscale (E7–9, E16–21, E29–31, E44–52) were selected from the forging and welding of both wrought iron and mild steel. The spheroids collected after some forging experiments are likely to be contamination from earlier experiments as they show considerable variation in microstructure and composition (Table 7). Sample E7 is cast iron (assumed to derive from overheating the tuyère), sample E8 is rich in titanium and probably derives from electric welding flux (*ie* activity prior to our experiments), sample E9 has a microstructure typical of burning

Table 6: Average composition of the experimental flake hammerscale samples.

	Na_2O	MgO	Al_2O_3	SiO_2	P_2O_5	SO_3	K_2O	CaO	TiO_2	MnO	Fe_3O_4
E1	0.5	0.1	0.9	2.1	0.5	2.0	<0.1	0.1	<0.1	<0.1	93.6
E2	0.5	0.2	1.7	3.9	0.4	1.6	0.1	0.1	0.2	<0.1	91.3
E3	0.7	0.1	1.1	4.5	0.7	2.4	0.2	0.5	0.2	<0.1	89.6
E4	0.3	0.1	0.7	1.7	0.4	2.2	<0.1	<0.1	<0.1	<0.1	94.4
E5	0.5	0.2	1.6	3.8	0.6	2.6	<0.1	0.2	0.1	<0.1	90.2
E6	0.2	<0.1	1.0	1.7	0.3	1.7	<0.1	<0.1	<0.1	<0.1	94.8
E22	0.1	0.2	0.6	1.2	0.4	0.7	<0.1	<0.1	0.1	<0.1	96.5
E23	0.5	0.1	1.5	4.3	0.7	1.8	<0.1	0.2	0.1	<0.1	90.6
E24	0.3	0.1	0.8	2.0	0.6	1.2	<0.1	0.1	<0.1	<0.1	94.6
E32	0.4	<0.1	0.9	1.7	<0.1	0.9	<0.1	0.1	<0.1	0.4	95.3
E33	0.5	<0.1	0.9	2.7	<0.1	1.7	0.1	0.1	<0.1	0.3	93.4
E34	0.3	<0.1	1.0	1.7	<0.1	1.1	<0.1	0.2	<0.1	0.6	94.9
E35	0.2	<0.1	1.1	2.7	<0.1	0.7	<0.1	0.1	<0.1	0.5	94.5
E36	0.4	<0.1	0.2	0.8	<0.1	1.1	<0.1	<0.1	<0.1	0.6	96.8
E37	0.4	<0.1	1.0	2.1	<0.1	0.8	<0.1	0.1	<0.1	0.5	95.0
E38	0.5	<0.1	0.6	3.6	<0.1	3.3	0.1	0.3	<0.1	0.5	90.8
E39	0.2	<0.1	0.5	1.3	<0.1	2.5	<0.1	<0.1	<0.1	0.4	94.8
E40	0.2	<0.1	0.6	1.6	<0.1	3.5	<0.1	<0.1	<0.1	0.5	93.4
E 41	0.9	<0.1	1.1	3.9	1.2	2.4	0.2	0.4	0.1	0.1	89.8
E42	0.9	0.2	1.4	3.8	<0.1	3.4	0.1	0.3	<0.1	0.5	89.3
E43	0.2	0.1	0.8	1.6	<0.1	0.4	<0.1	0.1	<0.1	0.4	96.0

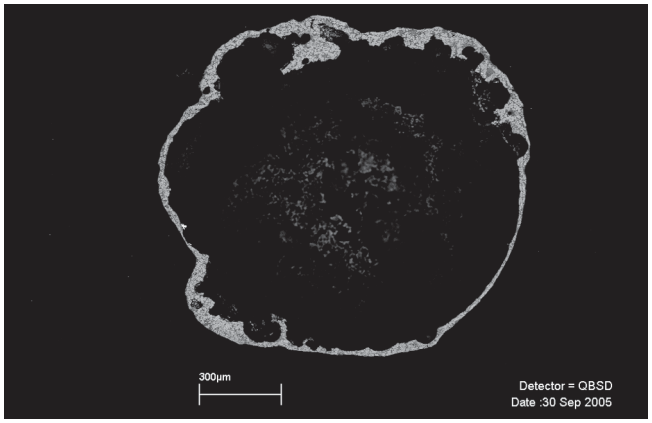

Figure 11: Backscattered electron image of a cross-section through sample E20 (spheroidal hammerscale) showing that a large proportion of it is hollow.

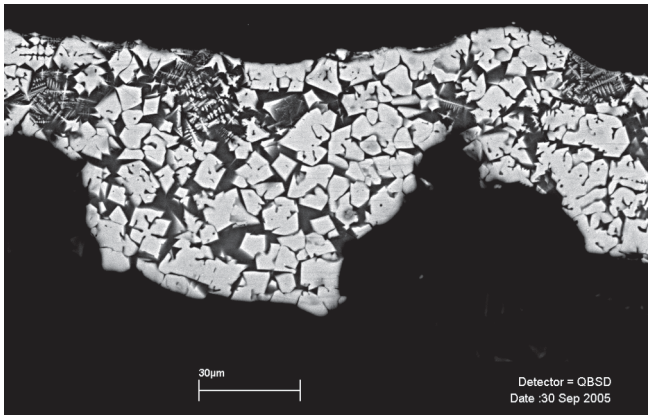

Figure 12: Backscattered electron image of a cross-section through sample E20 (spheroidal hammerscale) showing the largely euhedral nature of the iron oxide (magnetite).

(metallic core inside an oxide shell) and sample E18, which was collected after welding wrought iron, has a chemical composition typical of those produced by welding mild steel.

The other spheroids collected after welding wrought iron and mild steel all showed similar microstructures. Most were hollow (Fig 11) and comprized iron oxide (probably magnetite) in a fayalite or glassy matrix. Unlike the archaeological samples, however, the iron oxide is mainly present as small equiaxed euhedral grains rather than dendrites (Fig 12). The presence of euhedral grains rather than dendrites suggests a slower cooling rate compared to the archaeological examples. The manganese and phosphorus contents of these spheroids suggest that there are two compositional groups which appear to correspond to those produced from steel (high Mn) and wrought iron (high P).

Miscellaneous hammerscale

Miscellaneous hammerscale consists of material which is neither flake nor spheroid (cf Allen 1986). Examples had very variable shapes and sizes but many consist of half spheroids or sheets with a rather bubbly texture on

Table 7: Averaage composition of the experimental spheroidal hammerscale samples. The fragment of cast iron (E7) is not imcluded.

	Na_2O	MgO	Al_2O_3	SiO_2	P_2O_5	SO_3	K_2O	CaO	TiO_2	MnO	Fe_3O_4
E8	0.1	0.3	3.3	13.1	0.2	<0.1	1.3	3.8	53.8	9.3	14.7
E9	0.5	0.1	1.0	3.5	1.5	1.8	<0.1	0.3	<0.1	<0.1	91.2
E16	0.7	0.2	2.8	7.6	1.0	3.9	0.1	0.4	0.2	0.1	83.0
E17	0.7	0.3	2.5	9.5	0.9	0.2	0.1	0.5	0.1	<0.1	85.2
E18	0.8	0.4	5.7	15.3	<0.1	6.5	0.5	1.1	0.3	0.6	68.6
E19	1.0	0.4	3.8	14.3	1.9	<0.1	0.2	0.7	0.3	0.3	77.2
E20	1.1	0.5	4.2	15.7	1.2	<0.1	0.2	0.7	0.2	0.1	76.0
E21	1.2	0.4	4.0	14.1	1.1	<0.1	0.3	0.8	0.2	0.1	77.7
E29	0.6	0.4	3.1	8.0	0.6	0.1	<0.1	0.4	0.2	0.1	86.4
E30	0.3	0.1	1.1	4.9	1.6	0.8	<0.1	0.1	0.1	0.4	90.5
E31	0.8	0.3	4.0	12.8	0.8	4.8	0.2	0.6	0.2	0.1	75.4
E44	0.6	0.1	2.5	9.2	0.1	0.9	0.2	0.5	0.2	0.6	85.0
E45	0.6	0.3	3.1	9.8	0.1	0.2	0.3	0.7	0.1	0.5	84.3
E46	0.7	0.3	2.2	6.7	<0.1	2.7	0.2	0.3	0.2	0.5	86.1
E47	0.4	0.2	2.6	7.3	<0.1	2.5	0.1	0.3	0.1	0.8	85.5
E48	0.8	0.4	5.6	15.3	<0.1	1.0	0.4	1.0	0.3	0.6	74.4
E49	1.0	0.5	5.2	15.4	<0.1	0.1	0.5	1.0	0.3	0.5	75.4
E50	0.4	0.1	2.3	5.9	<0.1	2.4	0.1	0.3	0.1	0.5	87.7
E51	0.4	0.3	3.5	9.3	<0.1	1.0	0.2	0.4	0.2	0.6	84.0
E52	1.0	0.4	5.8	14.4	<0.1	<0.1	0.3	0.8	0.3	0.6	76.4

one surface. It makes up a small proportion of all of the hammerscale collected (7%) and was mostly associated with the working of wrought iron. Ten samples of miscellaneous hammerscale (E10–15, E25–28) were selected from the material collected during the forging and welding of wrought iron.

The miscellaneous hammerscale samples show considerable variation in microstructure with euhedral equiaxed grains, laths and dendrites present in a fayalite and/or glassy matrix. The compositions of the miscellaneous hammerscale samples show more similarities with the spheroidal hammerscale than the flake hammerscale (Table 8). Most of the miscellaneous hammerscale samples displayed significant phosphorus and low concentrations of manganese suggesting that all except E11 and E12 derived from wrought iron rather than mild steel.

Discussion of experimental hammerscale

The experimental hammerscale often displays similar results to those obtained from the archaeological material. Not all of the microstructures observed in the experimental hammerscale, however, can be found in the two groups of archaeological material. This is probably due to the nature of the metals and hearth used for the experiments. The limited availability of bloomery iron meant that 19th- or 20th-century puddled wrought iron was used instead of bloomery iron. In addition, the mild steel used in the experiments would be significantly different from steel produced by the bloomery process (whether produced directly or by subsequent carburisation). The hammerscale from the experiments tends to have much higher levels of phosphorus, sulphur and manganese than the archaeological material. It is likely that these elements derive from the non-metallic inclusions in the metals used for the experiments (see below). The experimental work employed a modern hearth (much larger than known archaeological examples) made of sheet metal rather than clay, and metallurgical coke. It is possible that different results would have been obtained if a small clay-lined hearth and charcoal fuel had been used.

The spheroidal and flake hammerscale usually have distinctive microstructures. The flake hammerscale consists of large (20–100μm) equiaxed grains (usually magnetite) in a fayalite or glassy matrix. The spheroidal hammerscale has the same phases but the magnetite is present as much smaller grains (<20μm) with a higher proportion of fayalite or glassy matrix. The iron oxide in the experimental spheroidal hammerscale does not have the same dendritic microstructure seen in the archaeological material.

The flake hammerscale tends to have a high iron content while all other types have a lower iron content and increased levels of a range of other oxides. The iron oxide is negatively correlated with most of the other oxides (*eg* Fig 6) and the other oxides are also often positively correlated with each other (*eg* Fig 7).

There are a number of different potential sources for the oxides other than the iron but some of these can be discounted for the experimental samples though not for the archaeological samples. The hearth used for the experiments was large and had no ceramic lining so this can be excluded as a source. In addition, no flux was used during the experiments. The two most likely sources of oxides other than iron for the experimental hammerscale are therefore the fuel ash (referred to as clinker when present as small vitrified masses) and the non-metallic inclusions in the metal. Samples of wrought iron and clinker were prepared and analysed (Table 9). A plot of phosphorus and manganese (Fig 13) indicates that the non-metallic (slag) inclusions in the metal made the most significant contribution, contributing a range of oxides to the formation of hammerscale (cf Tylecote 1962, 255). The

Table 8: Averaage composition of the experimental miscellaneous hammerscale samples.

	Na_2O	MgO	Al_2O_3	SiO_2	P_2O_5	SO_3	K_2O	CaO	TiO_2	MnO	Fe_3O_4
E10	0.5	0.1	1.8	6.1	0.9	4.5	<0.1	0.4	0.1	0.1	85.4
E11	0.3	0.1	1.8	9.7	2.7	3.2	0.1	0.4	0.3	0.6	80.7
E12	1.0	0.3	2.3	14.0	3.7	5.0	0.3	0.6	0.3	0.6	71.9
E13	1.0	0.3	2.9	10.9	1.7	5.5	0.2	0.6	0.2	0.3	76.5
E14	1.1	0.2	2.9	10.0	1.5	5.5	0.2	0.6	0.2	0.2	77.5
E15	1.2	0.2	2.6	8.9	1.0	3.5	0.2	0.4	0.1	0.2	81.7
E25	0.9	0.3	3.2	8.9	0.7	3.5	0.1	0.5	0.2	0.1	81.5
E26	0.4	0.1	2.4	9.4	0.8	4.3	0.2	0.4	0.1	<0.1	81.8
E27	0.2	0.2	2.4	8.1	0.7	4.2	0.2	0.4	0.2	<0.1	83.6
E28	0.5	0.2	2.4	7.3	0.7	4.0	0.1	0.4	0.2	<0.1	84.1

Table 9: Averaage composition of experimental hammerscale produced from wrought iron, slag inclusions in the wrought iron, and clinker.

	Na_2O	MgO	Al_2O_3	SiO_2	P_2O_5	SO_3	K_2O	CaO	TiO_2	MnO	Fe_3O_4
Flake	0.4	0.1	1.1	2.8	0.5	1.8	<0.1	0.1	0.1	<0.1	92.9
Spheroid	0.9	0.4	3.5	12.2	1.2	0.8	0.2	0.6	0.2	0.2	79.8
Slag inclusions	<0.1	<0.1	2.3	13.7	7.1	0.8	<0.1	0.3	0.5	1.6	73.4
Clinker	1.5	1.7	23.4	55.2	<0.1	0.1	3.0	1.1	1.3	<0.1	12.6

relative importance of slag inclusions is reinforced by the compositional differences between the hammerscale produced by working wrought iron and steel. Unfortunately, no sample of the mild steel used in the experiments was retained and the later collection of several samples of mild steel stock from West Dean showed a range of compositions with a variety of non-metallic inclusions present, including manganese sulphides, manganese silicates and aluminium-calcium-silicates.

Modelling the formation of hammerscale

Flake hammerscale

The formation of oxidized surfaces on iron and iron alloys has been the subject of intensive study (*eg* Birosca *et al* 2004; Chen and Yeun 2003; Iordanova *et al* 2000). The nature of the oxide surface that forms on iron depends primarily on temperature. Below 570ºC the oxide surface contains two layers, an inner layer of magnetite (Fe_3O_4) and an outer layer of haematite (Fe_2O_3); above 570ºC the oxide surface contains three layers, a thick inner layer of wüstite (FeO), a thin intermediate layer of magnetite, and an extremely thin outer layer of haematite. The wüstite layer is the thickest as the 'diffusion coefficient of iron in wüstite is much greater than in magnetite and the diffusion of oxygen and iron through the hematite layer is extremely slow' (Chen and Yuen 2003, 435). While the wüstite layer is thickest during high-temperature oxidation, it is not thermodynamically stable below 570ºC and 'magnetite precipitation within the wüstite layer is essentially inevitable' (*ibid*, 436). Magnetite precipitation depends primarily on cooling rate but appears to be extensive in both the archaeological and experimental samples examined here.

The initial growth of oxidized surfaces on hot iron is fast but that rate of growth slows as the oxide layer becomes thicker, *ie* the oxidation of the metal is a diffusion-controlled reaction (Fig 14). Experimental work has also shown that the thickness of the oxide layer (for a given time) increases with temperature (Fig 15). Iron becomes softer as it is heated and this is particularly noticeable above 910°C when ferrite is transformed into austentite. Blacksmiths would probably avoid excessively high temperatures when shaping iron as these would accelerate oxidation and could even lead to combustion. However, higher temperatures (1100–1300°C) would

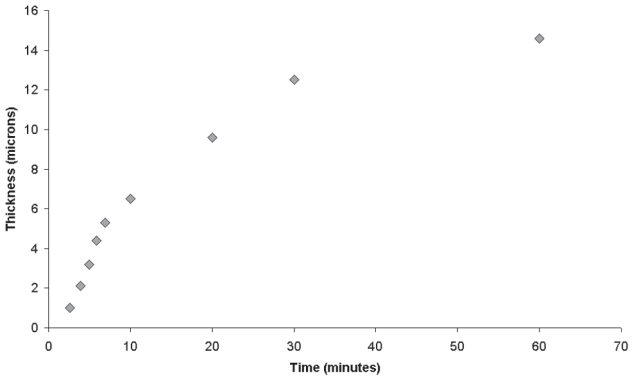

Figure 14: The thickness of oxide layer formed on low-carbon steel at 600ºC (after Iordanova et al 2000, fig 3).

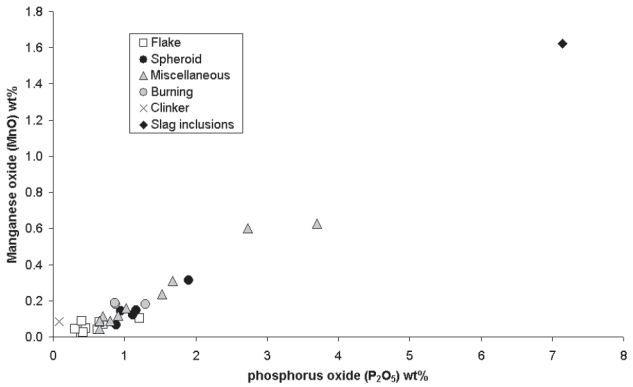

Figure 13: Phosphorus oxide v. manganese oxide for hammerscale and other materials from working wrought iron.

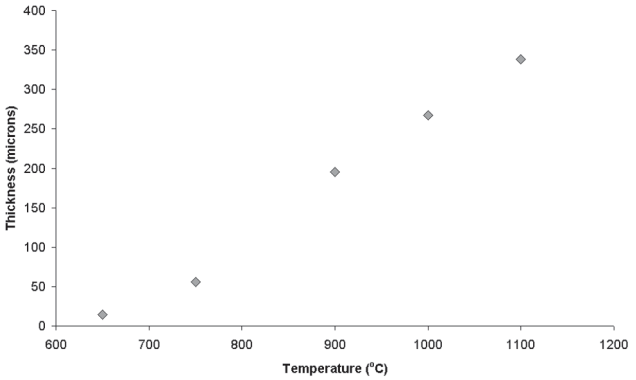

Figure 15: The thickness of oxide layer formed on carbon-free iron after 60 minutes (after Birosca et al 2004).

have been employed when welding. The duration of heating would depend largely on the mass of iron being heated but this would rarely have exceeded 10 minutes. Assuming a heating temperature of 1000ºC and a heating time of 5 minutes, the thickness of scale produced on carbon-free iron would be approximately 50μm (Birosca *et al* 2004, fig 2). Most archaeological examples of flake hammerscale are substantially thicker than 50μm but often display a series of distinct layers some of which are roughly 50μm thick (Fig 3). It is possible that flake hammerscale often grew *in situ* through several heats.

When considering the growth of flake hammerscale during heating prior to fire-welding, the higher temperature and longer duration of the heating will produce thicker layers of flake hammerscale. Assuming a temperature of 1200ºC and duration of 10 minutes, the thickness of the scale produced on carbon-free iron would be approximately 300μm (Birosca *et al* 2004, fig 2).

Spheroidal hammerscale

The experimental forging and fire-welding of wrought iron and mild steel has shown that spheroidal material is produced during fire-welding and during the combustion of these metals. While the combustion of ferrous alloys is of considerable interest in modern industries there appears to be no scientific literature which addresses the formation of spheroidal oxide particles during fire-welding. The limited literature on the combustion of iron usually focuses on oxygen-rich environments (Bolobov 2001; Charles and Chater 1978; Sato *et al* 1995; Steinberg *et al* 1992) which may not be entirely applicable to a blacksmith's hearth. In addition, much of the current research focuses on the combustion of iron in low gravity environments (the goal being to prevent the combustion of components of rockets and other space vehicles).

As iron is heated in an atmosphere containing oxygen, an oxide layer grows at the surface as described above. This oxide layer provides a degree of protection for the underlying metal but only while the oxide remains solid. Once the oxide surface melts, it ceases to protect the metal in the same way as oxygen can diffuse quickly through the molten oxide. In additional the molten oxide can flow and so may leave areas of the unoxidized metal exposed. As result, the metal will oxidize very rapidly — it combusts. The bulk of the oxide surface on iron is made up of wüstite which melts at 1371ºC (the other oxides form a small proportion of the surface layer and have higher melting temperatures) but experimental work by Bolobov (2001) and Sato *et al* (1995) has shown that the combustion of iron and mild steel occurs from 1250ºC. Unfortunately, the iron combustion literature contains few observations on the form of the material resulting from combustion. As the burnt material moves away from the metal it will be in a liquid state and so will have a high surface tension. Therefore it is likely that the material will form spheroids which, due to the high surface area, will cool quickly and so should retain this shape.

Research by Charles and Chater (1978) showed that hollow slag droplets are produced during the oxygen cutting of iron. This technique relies on preheating the metal and then introducing a stream of oxygen. The heated iron reacts with the oxygen generating more heat, leading to a limited form of combustion which cuts through the metal. Charles and Chater observed that the slag collected from the bottom of their experimental cuts 'are always in the form of hollow droplets when cold' (*ibid*, 166) and suggest that the hollow form is due to the liberation of gas during cooling but before the outer surface solidifies. More recent experiments by Steinberg and colleagues have demonstrated that oxygen solubility in iron and its oxides increases at high temperatures but that this is released on cooling to form voids (Steinberg *et al* 1998). This mechanism may explain the formation of hollow spheroids during fire-welding.

Conclusions

The SEM images of flake hammerscale from archaeological contexts and the experiments have shown that they usually have relatively large equiaxed iron oxide grains with a small amount of silicate material along grain boundaries. It is likely that a single period of heating for ordinary forging would produce an oxide layer 50μm thick, while heating prior to welding would produce a layer 300μm thick. Many archaeological samples of flake hammerscale display a series of layers which may indicate more than one period of heating before the flake became detached. The examination of the experimental flake hammerscale showed no significant differences in thickness between that collected from forging experiments and that collected from welding experiments.

The spheroidal hammerscale from archaeological contexts has a more variable microstructure than the flakes but most commonly this consists of a hollow spheroid, the skin of which contains fine iron oxide dendrites in a silicate matrix. Unlike the flake hammerscale, spheroidal hammerscale has clearly been molten at some stage. The experimentally produced spheroidal hammerscale rarely had a microstructure comparable with the archaeological specimens (the iron oxide was generally euhedral rather than dendritic), possibly due to the nature of the experiment and the materials used.

An examination of the chemical composition of the various types of hammerscale suggests that non-metallic inclusions in the parent metal make a significant contribution, especially to the spheroidal material. The compositions of the archaeological samples provide no evidence for the use of a separate flux (and the experimental welding was achieved without the use of a flux).

The collection of hammerscale produced at each stage of the experiments shows that spheroidal hammerscale is mainly associated with fire-welding. The high-speed digital video confirms that spheroids are produced by welding, and that they emerge from the weld line as an amorphous stream of material which coalesces into a series of spheroids within 0.03 seconds. The deliberate burning of iron and steel was relatively easily achieved and showed that spheroidal material could be produced by this process. Most of these combustion spheres could be easily distinguished from welding spheres by the presence of a small metallic iron core.

Acknowledgements

We would like to thank Vincent Guichard and all the staff and colleagues at the Centre Archéologique Européen de Mont Beuvray, Glux en Glenne, Saône et Loire, France who provided access to Mont Beuvray for the archaeological teams from English Heritage and the University of Southampton. The excavation of the 1st-century BC blacksmith's workshops allowed the collection of large quantities of hammerscale. We are grateful to Howard Brooks of Colchester Archaeological Trust who provided the samples of hammerscale from 79 Hythe Hill, Colchester. We would like to thank Tonny Bentjes and West Dean College who provided access to the blacksmithing workshops (and lunch!). Andrew Breese (one time tutor on the blacksmithing courses) provided initial guidance on how to forge and weld iron and steel, and continued to supervise the experimental stages. Eleanor Blakelock and Vanessa Fell provided assistance during the experimental forging and welding at West Dean. Much of the interpretation has emerged through discussions with colleagues, in particular Ted Steinberg, Gerry McDonnell, Vincent Serneels, Tim Young, Chris Salter and Jim Charles.

References

Allen J R L 1986, 'Interpretation of some Romano-British smithing slag from Awre in Gloucestershire', *Historical Metallurgy* 20, 97–104.

Bayley J, Dungworth D and Paynter S 2001, *Archaeometallurgy* (London: English Heritage Guidelines 2001/01).

Birosca S, Dingley D and Higginson R L 2004, 'Microstructural and microtextural characterization of oxide scale on steel using electron backscatter diffraction', *Journal of Microscopy* 213, 235–40.

Bolobov V I 2001, 'Conditions for ignition of iron and carbon steel in oxygen', *Combustion, Explosion, and Shock Waves* 37, 292–296.

Brooks H 2000, 'Excavations at 79 Hythe Hill, Colchester 1994–5', *Essex Archaeology and History* 31, 112–124.

Charles J A and Chater W J B 1978, 'Oxygen cutting', *Metals Technology* 5, 163–175.

Chen R Y and Yeun W Y D 2003, 'Review of the high-temperature oxidation of iron and carbon steels in air or oxygen', *Oxidation of Metals* 59, 433–68.

CSIRA 1952, *The Blacksmith's Craft* (Salisbury).

Forster R H and Knowles W H 1910, 'Corstopitum: report on the excavations in 1909', *Archaeologia Aeliana* 6, 205–272.

Forster, R H and Knowles, W H 1913, 'Corstopitum: report on the excavations in 1912', *Archaeologia Aeliana* 9, 230–280.

Guichard V, Barral P, Beck P, Bonenfant P-P, Boyer F, Creighton J, Dhennequin L, Dominguez-Arranz A, Dufay-Flouest A, Dungworth D, Durost S, Gran-Aymerich J, Gruel K, Guillaumet J-P, Hamm G, Haselgrove C, Jouffroy-Bapicot I, Lambert G, Laszlovsky J, Lowther P, Luginbühl T, Monna F, Olmer F, Paris P, Paunier D, Petit C, Popovitch L, Richard H, Rieckhoff S, Schubert F, Szabó M, Toledo I Mur A, Urban O, Vitali D and Wiethold J 2003, 'Un aperçu des acquis récents des recherches sur l'oppidum de Bibracte (1997–2002)', *Revue Archéologique de l'Est* 52, 45–90.

Iordanova I, Surtchev M, Forcey K S and Krastev V 2000, 'High-temperature surface oxidation of low-carbon rimming steel', *Surface and Interface Analysis* 30, 158–160.

McDonnell G 1984, 'The study of early iron smithing residues', in B G Scott and H Cleere (eds), *Crafts of the Blacksmith* (Belfast), 47–52.

McDonnell G 1986, The classification of early iron working slags, unpublished PhD thesis, University of Aston, Birmingham.

Mills A and McDonnell G 1992, *The identification and analysis of the hammerscale from Burton Dassett Warwickshire* (London: Ancient Monuments Laboratory Report 47/1992).

Sato J, Ohtani H and Hirano T 1995, 'Ignition process of a heated iron block in high-pressure oxygen atmosphere', *Combustion and Flame* 100, 376–383.

Sim D 1998, *Beyond the Bloom* (Oxford: BAR IS 725).

Simpson F G and Richmond I A 1941, 'The Roman Fort on Hadrian's Wall at Benwell', *Archaeologia Aeliana* 19, 1–43.

Starley D 1997, *The analysis of slag and other metalworking debris from Creeton Quarry, Lincs* (London: Ancient Monuments Laboratory Report 99/1997).

Steinberg T A, Mulholland G P, Wilson B and Benz F J 1992, 'The combustion of iron in high-pressure oxygen', *Combustion and Flame* 89, 221–228.

Steinberg T A, Kurtz J and Wilson D B 1998 'The solubility of oxygen in liquid iron oxide during the combustion of iron rods in high-pressure oxygen', *Combustion and Flame* 113, 27–37.

Tylecote R F 1962, *Metallurgy in Archaeology* (London).

Tylecote R F and Owles E 1960, 'A second-century iron smelting site at Ashwicken, Norfolk', *Norfolk Archaeology* 32, 142–162.

Unglik H 1991, 'Observations on microscopic smithing residues from Bixby Blacksmith Shop, Barre Four Corners, USA 1824–55', *Historical Metallurgy* 25, 92–98.

The authors

David Dungworth obtained a degree in ancient history and archaeology from the University of Birmingham in 1991 and a PhD (*Iron Age and Roman Copper Alloys from Northern Britain*) from the University of Durham in 1995. Since 1999 he has been employed by English Heritage as a materials scientist.
Address: English Heritage, Fort Cumberland, Eastney, Portsmouth PO4 9LD.
e-mail: david.dungworth@english-heritage.org.uk

Roger Wilkes worked in the aerospace components industry as an electrical technician where he obtained City and Guilds 280/281 certificates. He specialized in the SEM analysis of electronic component failure. Since 2000 he has been the instrument technician for the English Heritage Technology Team.
Address: English Heritage, Fort Cumberland, Eastney, Portsmouth PO4 9LD.
e-mail: roger.wilkes@english-heritage.org.uk